Elasticity and porosity in human cortical bone: models and experiments

(Elasticité et porosité de l'os cortical humain : modèles et expériences)

M. GRANKE[a], Q. GRIMAL[a], W.J. PARNELL[b], A. SAÏED[a], F. PEYRIN [c], P. LAUGIER[a]

a. UPMC Univ Paris06, UMR 7623, Laboratoire d'Imagerie Paramétrique, 75005 Paris; CNRS, UMR 7623, Laboratoire d'Imagerie Paramétrique, 75005 Paris
b. School of Mathematics, Alan Turing Building, University of Manchester, Manchester (UK)
c. CREATIS INSERM U1044; CNRS 5220; INSA Lyon; Université de Lyon, 69621 Villeurbanne Cedex; ESRF, 38043 Grenoble

Résumé :

A l'échelle millimétrique, l'os cortical est vu comme une matrice minéralisée traversée de pores (canaux de Havers). Nous avons mesuré la porosité et l'élasticité de 21 échantillons (10 donneurs) et nous avons montré que la rigidité de la matrice a une influence mineure sur l'élasticité apparente. Ces données permettent pour la première fois une analyse critique des modèles de changement d'échelle (homogénéisation asymptotique, Mori-Tanaka, auto-cohérent, bornes de Hashin-Shtrikman). La comparaison de nos mesures avec les prédictions des modèles indique que l'os cortical peut en première approche être modélisé avec des propriétés du tissu fixes et une porosité échantillon-dépendante.

Abstract:

At the millimeter scale, cortical bone can be considered as a mineralized matrix pervaded by cylindrical pores (Haversian canals). We measured the porosity and the elasticity of 21 samples (10 donors) and we showed that the matrix stiffness has a minor influence on the apparent elasticity. These data allow for the first time a critical analysis of multiscale models (asymptotic homogenization, Mori-Tanaka, self consistent, Hashin-Shtrikman bounds). The comparison of our measurements with the predictions of the models indicates that, in a first approximation, cortical bone can be modeled with fixed matrix properties and a sample-dependent porosity fraction.

Mots clefs : os cortical humain, élasticité, porosité, homogénéisation, ultrasons

1 Introduction

Bone is a multiscale biocomposite whose structure and mechanical properties at one level determine the properties of the subsequent one. Despite numerous studies dedicated to the assessment of cortical bone mechanical properties, some questions remain open regarding the determinants of cortical bone elasticity. A clear understanding of elasticity is needed for the modeling of the macroscopic (organ scale) behavior of bones, the investigation of structural-functional relationships (remodeling) and the development of new in vivo assessment methods of bone quality.

At the mesoscale (2-10 millimeters, [1]), cortical bone can be described as a two-phase composite material, a dense mineralized matrix and a soft phase, i.e. Haversian canals and resorption cavities (referred to as vascular porosity) containing fluid and soft tissues. It has been suggested that porosity is an important determinant of the mesoscopic bone properties [2,3]. On the other hand, the impact of the bone matrix properties on the bone mesoscopic elasticity is a matter of debate in the literature. There has yet to be a conclusive investigation as to whether only the variations of porosity should be accounted for or if the bone matrix properties are a critical factor to predict the variations of the mesoscopic effective elasticity. To address this question, we measured on the same samples from ten donors (aged women): the porosity, the bone matrix elasticity (reflected in acoustical impedance values) and the mesoscopic anisotropic elastic coefficients [4]. We found that, for the elderly population, the elastic properties of the mineralized matrix do

not undergo large variations among different samples and that the variations in porosity account for most of the variations of mesoscopic elasticity, at least when the analyzed porosity range is large.

Micromechanical models are useful as a means of testing how changes of the bone microscale properties affect its mesoscopic (or macroscopic) behavior, for hypothesized organizational patterns. Various homogenization schemes have been applied to cortical bone to model the effect of the vascular porosity on mesoscopic elasticity (e.g. [5-10]). However, to be validated, these models should be compared to comprehensive experimental results obtained on the same samples from a large collection, data not found in existing literature.

Our objective was to test whether bone can be modeled as a two-phase composite: a mineralized matrix pervaded by pores. We hypothesize that the mineralized matrix properties are only responsible for a small fraction of the variations of mesoscale elasticity and that the variation of vascular porosity is mainly responsible for these variations. The originality of our work is that (1) for the first time, we assess the "composite model" of bone with experimental data; (2) we compare the predictions of the main classical homogenization schemes to determine which is the most appropriate for bone.

2 Experiments

Fresh bone specimens were prepared from a collection of ten left femoral mid-diaphysis of female cadavers (age = 81.3 ± 8.7 [66-98] years). Twenty-one samples (nominally 5x5x7 mm^3) were harvested from different anatomical quadrants (lateral, medial, posterior) in order to maximize the variability of bone properties. The faces of the samples were oriented according to the radial (1), circumferential (2), and longitudinal (3) axes defined by the anatomic shape of the femoral diaphysis. The samples were defatted then stored in gauze soaked in saline solution at 4°C prior to measurements.

Mesoscale elasticity was determined from the wave velocities and apparent mass measurements. The ultrasonic (US) wave velocities were measured using a well-established pulse transmission method [11] with a pair of frequency matched contact transducers. Longitudinal (2.25 MHz) and shear (1 MHz) waves were used to measure the diagonal terms of the stiffness tensor (C_{11}, C_{22}, C_{33} for the longitudinal and C_{44}, C_{55}, and C_{66} for the shear). Measurement errors were assessed by repeating longitudinal and shear wave velocity measurements on one specimen for five consecutive days with intermediate repositioning. The reproducibility was 3.2% and 4.7% for the mesoscopic longitudinal and shear stiffness coefficients, respectively.

50-MHz-Scanning Acoustic Microscopy (SAM, [12]) provided calibrated acoustical impedance maps with a lateral resolution of 30 µm for all six faces of each sample. After an image processing to separate the pores and the mineralized matrix, the porosity *p* was defined as the average relative pore area in the faces in the 1-2 planes. The porosity error was evaluated on ten samples by comparing the porosity as obtained by SAM (*p*) and the porosity as measured on the sample 3D-reconstruction (voxel 5 μm^3) using synchrotron radiation micro-computed tomography (ESRF, Grenoble, France). The comparison led to an average error of 0.8% on the estimate of the porosity *p*. The porosity was found to be 13.5 ± 6.8 % covering a wide range of values [3-27%].

3 Micromechanical models

First, a model of cortical bone elasticity based on asymptotic homogenization (AH) [9] was used to test a model accounting for porosity variations only. Briefly, the model hypothesizes that cortical bone can be regarded as a homogeneous transversely isotropic (TI) matrix pervaded by infinite cylindrical pores, periodically distributed within the matrix material (specifically on a hexagonal lattice). The material in pores is assumed to behave like bulk water (undrained), that is, bulk modulus and Poisson ratio are set to 2.3 GPa and 0.49, respectively. The (TI) stiffness tensor C^m of the bone matrix was identical for all samples and chosen so that the distance between the experimental points and model was minimum (C_{11}^m = 26.8 GPa, C_{33}^m = 35.1 GPa, C_{44}^m = 7.3 GPa, C_{66}^m = 5.8 GPa, and C_{13}^m = 15.3 GPa). Once converted into engineering moduli (E_T = 16.5 GPa, E_L = 24.0 GPa, G_T=5.8 GPa, G_L = 7.3 GPa), the elasticity values assigned to the bone matrix were found to be consistent with the literature [13].

The comparison between the mesoscopic stiffness coefficients determined from experiments and the AH model (Fig. 1) showed that the modeling of bone as a composite material provided good estimates of mesoscopic stiffness variations (RMSE: C_{11}=1.0 GPa, C_{22}=1.2 GPa, C_{33}=1.7 GPa, C_{44}=0.3 GPa, C_{55}=0.4 GPa,

C_{66}=0.3 GPa). Note that, since the homogenized stiffness tensor C^{AH} is (TI), the experimental values C_{11}, C_{22}, C_{33}, C_{44}, C_{55}, C_{66} were compared to $C_{11}^{AH}, C_{11}^{AH}, C_{33}^{AH}, C_{44}^{AH}, C_{44}^{AH}, C_{66}^{AH}$ respectively.

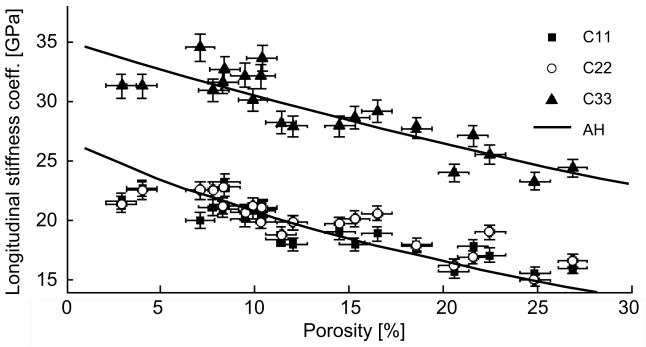

FIG. 1 – Longitudinal stiffness coefficients versus porosity. Vertical error bars represent the experimental errors on the C_{ii} (reproducibility). Horizontal error bars represent the error on the porosity (exactitude). The lines display the AH stiffness coefficients. Similar trends are obtained for shear coefficients (data not shown).

Despite a strong correlation, fluctuations in the stiffness coefficients could not be fully explained by the porosity variations, even after taking into account the measurement errors ($\Delta C_{11}=\Delta C_{22}$=0.6 GPa, ΔC_{33}=0.9 GPa, $\Delta C_{44}=\Delta C_{55}$=0.3 GPa, ΔC_{66}=0.2 GPa) (Fig. 1). Two possible sources for this variability were investigated: the orientation of the sample and the bone matrix stiffness.

A potential experimental error arises due to potential misalignment with the anatomical bone axis during the cutting of the sample. The misalignment is not expected to be more than 10°. Applying a rotation to the homogenized (AH) stiffness tensor around the axis 1 and 2 for ± 10° tested the influence of such misalignment (Fig. 2). The mean variation of (AH) stiffness coefficients caused by a 10° misalignment would be on average ΔC_{11}=0.2 GPa, ΔC_{33}=0.4 GPa, ΔC_{44}=0.1 GPa, and ΔC_{66}=0.05 GPa, which is far inferior to the observed fluctuations.

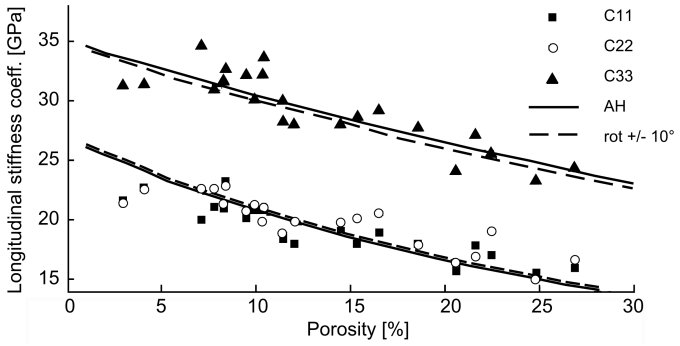

FIG. 2 – Longitudinal stiffness coefficients versus porosity. The solid lines display the AH stiffness coefficients. The doted lines show the influence of a ±10° rotation around the axis 1 and 2. Similar trends are obtained for shear coefficients (data not shown).

In this work, identical matrix stiffness was assigned to all the samples. In fact, with a coefficient of variation of the matrix impedance inferior to 5%, experimental results suggested that elastic properties did not undergo large variations in different samples. To evaluate the influence of the matrix stiffness on the homogenized stiffness, the (AH) stiffness coefficients were computed for varying bone matrix stiffness (± 5%). This induced an average variation of ΔC_{11}= ± 0.8GPa, ΔC_{33}= ± 1.3GPa, ΔC_{44}= ± 0.3GPa, and ΔC_{66}= ± 0.2GPa (Fig. 3).

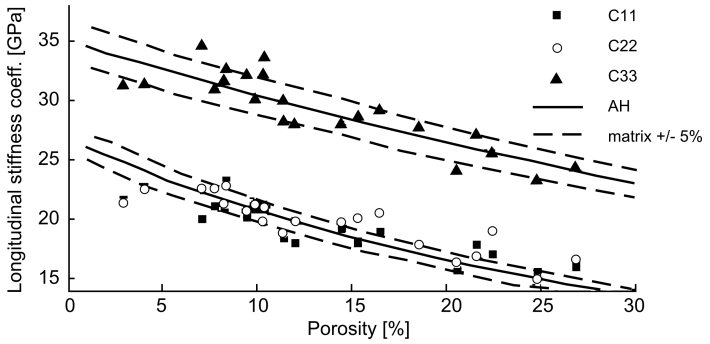

FIG. 3 – Longitudinal stiffness coefficients versus porosity. The solid lines display the AH stiffness coefficients. The doted lines show the influence of a ±5% variation of the matrix stiffness. Similar trends are obtained for shear coefficients (data not shown).

If the AH model only accounts for the porosity and the stiffness of the two phases (pores and bone matrix), other models based on Eshelby's matrix-inclusion problems [14] allow considering additional information, such as the shape of the inclusion and its interaction with the matrix. Here, three formulations of this approach were applied to cortical bone while considering a transversely isotropic inclusion, i.e. a spheroid:

a) The Hashin-Shtrikman (HS) bounds provide bounds on the components of the homogenized stiffness tensor.
b) The Mori-Tanaka scheme (MT) is used to represent a composite material (contiguous matrix with inclusions). In the case of bone, the inclusions are the pores embedded in the mineralized bone matrix.
c) The self-consistent approach (SC) considers the material as a disperse arrangement of the phases, i.e. the phases interpenetrate each other (typical for polycrystals).

In the three models, the same stiffness tensors for the two phases (bone matrix and pores) as for the AH model are used. For the self-consistent scheme, the bone matrix is modeled with a spherical inclusion.

A common parameter to these three models is the definition of the pores inclusion shape. Considering a TI spheroidal inclusion (i.e. with a circular cross-section), we tested the influence of the aspect ratio δ (= length/diameter) of the pores. For the three models, MT, SC as well as the HS bounds, the homogenized stiffness coefficients remain constant when the aspect ratio was greater than 10 (Fig. 4). Considering that, in human femoral mid-diaphysis, the osteon length was found to be 4 mm on average, 10 mm maximum [15], and the average haversian canals diameter was 150±119 µm [57-457] [16], with significantly greater values in elderly women, we can assume that δ resides in the range [25-80].

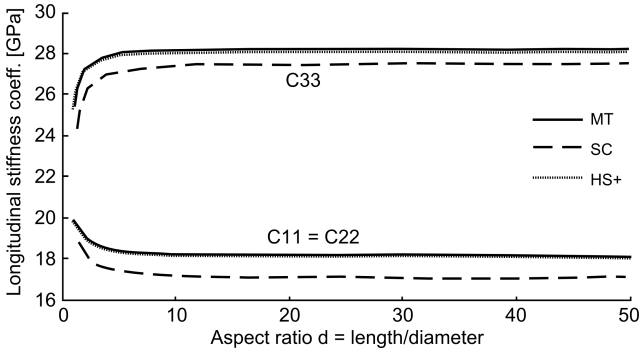

FIG. 4 – Longitudinal stiffness coefficients as obtained from micromechanical models (MT, SC, HS+) versus the pores aspect ratio (= length/diameter). Similar trends are obtained for shear coefficients (data not shown).

The aspect ratio of the pores was set to 25. The homogenized stiffness as obtained with HS [17], MT, and SC, were compared to the experimental stiffness coefficients. Regarding the HS bounds (Fig. 5), the experimental stiffness coefficients were close to the upper bound. The AH and MT models predicted well the mesoscopic stiffness coefficients, whereas the SC scheme displayed a stronger decrease with increasing porosity (Fig. 6).

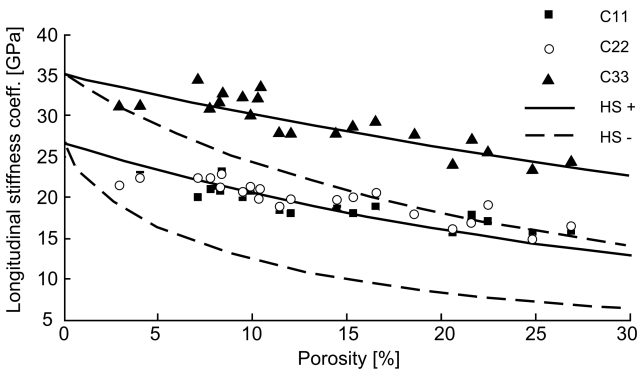

FIG. 5 – Longitudinal stiffness coefficients versus porosity. The solid and dotted lines display the upper and lower HS bounds for the homogenized stiffness coefficients, respectively. Similar trends are obtained for shear coefficients (data not shown).

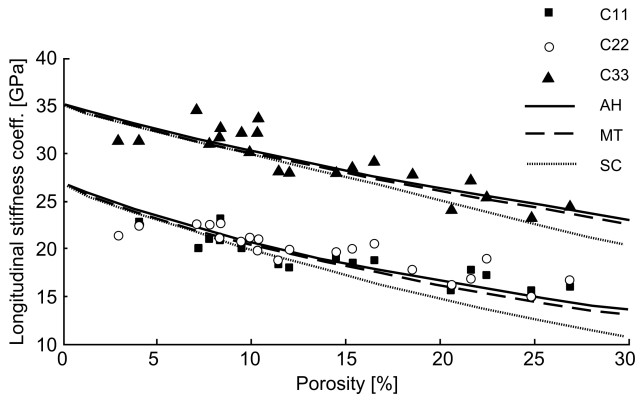

FIG. 6 – Longitudinal stiffness coefficients versus porosity. The lines display the stiffness coefficients as obtained from micromechanical models (AH, MT, SC). Similar trends are obtained for shear coefficients.

4 Discussion and conclusion

This work is an extension of a previous experimental study [4], in which the porosity, the bone matrix elasticity (as reflected by the acoustic impedance), and the anisotropic mesoscopic stiffness coefficients were measured on the same samples (twenty-one from ten donors). Experimental results suggested that the variations in vascular porosity accounts for most of the variations of mesoscopic elasticity, at least when the analyzed porosity range is large (3-27% in this work).

The same mineralized matrix stiffness tensor C^m was assigned for all models. We could have calculated the optimized C^m for the different methods but our objective was to compare the decreasing rate of stiffness versus porosity predicted in the different models.

Adding the experimental error measurements to the potential error in the alignment does not allow one to explain entirely the observed fluctuations of the stiffness coefficients around the AH model predictions. On the other hand, a change in the matrix elasticity could explain the remaining gap between the experimental data and the model.

The SC model is commonly used to model composite materials with intertwined phases. The results confirmed that this representation is not adapted for the pores, clearly distinguishable from the matrix.

The MT and AH models provided better fit than the self-consistent method. Note that, the AH and MT models displayed very close results, indicating that the pores can be modeled as infinite cylinders.

Since all the stiffness coefficients of the bone matrix are superior to that of the pores, the upper HS bound was, by definition, confounded with the MT predictions.

To conclude, although most of the models that have been proposed for cortical bone were based on several steps of homogenization and many variables, we show that a simple model such as a two-phase composite material is a suitable representation for cortical bone. Precisely, cortical bone can be modeled, in a first approximation, with fixed matrix properties and a sample-dependent porosity fraction. The results also suggest that a precise sample-specific model of a cortical sample should nevertheless account for the elasticity of the bone matrix.

The outcome of this fundamental study provides valuable insights for predicting the variations of bone

elasticity at the millimeter scale. In particular, this is of first interest for modeling the macroscopic mechanical behavior of bones, e.g. using personalized finite element models or investigating structure-functional relationships, e.g. the effect of bone remodeling on local elasticity.

References

[1] Grimal Q., Raum K., Gerisch A., Laugier P., A determination of the minimum sizes of representative volume elements for the prediction of cortical bone elastic properties. Biomechanics and Modeling in Mechanobiology, 2011, doi:10.1007/s10237-010-0284-9.
[2] Rho J.Y., Zioupos P., Currey J.D., Pharr G.M., Microstructural elasticity and regional heterogeneity in human femoral bone of various ages examined by nanoindentation. Journal of Biomechanics, 35, 189-198, 2002.
[3] Dong X.N., Guo X.E., The dependence of transversely isotropic elasticity of human femoral cortical bone on porosity. Journal of Biomechanics, 37, 1281-1287, 2004.
[4] Mouchet M., Nauleau P., Grimal Q., Saïed A., Laugier P., Ultrasonic assessment of the determinants of human cortical bone elasticity: relative contributions of Haversian porosity and mineralized matrix, 2010 IEEE International Ultrasonics Symposium proceedings, 2010.
[5] Hellmich C., Ulm F.J., Dormieux L., Can the diverse elastic properties of trabecular and cortical bone be attributed to only a few tissue-independent phase properties and their interactions? Biomechanics and Modeling in Mechanobiology, 2, 219-238, 2004.
[6] Dong X.N., Guo X.E., Prediction of cortical bone elastic constants by a two-level micromechanical model using a generalized self-consistent method. Journal of Biomechanical engineering,128, 309-316, 2006.
[7] Pedroi-Racila M., Crolet J.M., Human cortical bone: the SiNuProS model. Computer Methods in Biomechanics and Biomedical Engineering, 11, 169-187, 2008.
[8] Deuerling J.M., Yue W., Espinoza Orias .A., Roeder R.K., Specimen-specific multi-scale model for the anisotropic elastic constants of human cortical bone. Journal of Biomechanics, 42, 2061-2067, 2009.
[9] Parnell W.J., Grimal Q., The influence of mesoscale porosity on cortical bone anisotropy. Investigations via asymptotic homogenization. Journal of the Royal Society Interface, 6, 97-109, 2009.
[10] Grimal Q., Rus G., Parnell W.J., Laugier P., A two-parameter model of the effective elastic tensor for cortical bone. Journal of Biomechanics, in press, 2011.
[11] Espinoza Orias A.A., Deuerling J.M., Landrigan M.D., Renaud J.E., Roeder R.K., Anatomic variation in the elastic anisotropy of cortical bone tissue in the human femur. Journal of the mechanical behaviour of biomedical materials, 2, 255-263, 2009.
[12] Saïed A., Raum K., Leguerney I., Laugier P., Spatial distribution of anisotropic acoustic impedance assessed by time-resolved 50-MHz scanning acoustic microscopy and its relation to porosity in human cortical bone. Bone, 43, 187-194, 2008.
[13] Rho J.Y., Roy II M.E., Tsui T.Y., Pharr G.M., Elastic properties of microstructural components of human bone tissue as measured by nanoindentation. Journal of Biomedical Materials Research Part A, 45, 48-51, 1999.
[14] Eshelby J.D., The determination of the elastic field of an ellipsoidal inclusion, and related problems. Proceedings of the Royal Society of London A, 241, 376-396, 1957.
[15] Cooper D.M.L., Thomas C.D.L., Clement J.G., Hallgrimsson B, Three-dimensional microcomputed tomography imaging of basic multicellular unit-related resorption spaces in human cortical bone. The Anatomical Record part A, 228A, 806-816, 2006.
[16] Cooper D.M.L., Thomas C.D.L., Clement J.G., Turinsky A.L., Sensen C.W., Hallgrimson B., Age-dependent change in the 3D structure of cortical porosity at the human femoral midshaft. Bone, 40, 957-965, 2007.
[17] Parnell W.J., On the construction of the Hashin-Shtrikman bounds for transversely isotropic elastic composites. Quarterly Journal of Mechanics and Applied Mathematics, in preparation for submission, 2011.